Phyto-emulsomes as a novel nano-carrier for morine hydrate to combat leukemia: In vitro and pharmacokinetic study

Phyto-Emulsomes as a novel nano-carrier for Morine Hydrate to combat leukemia: In vitro and pharmacokinetic study

Rabab Kamel[a] , Mona M. AbouSamra*[a], Sherif M. Afifi[b] and Asmaa F. Galal[c]

[a]Pharmaceutical Technology Department, Pharmaceutical and Drug Industries Institute, National Research Centre, Cairo 12622, Egypt.

[b]Pharmacognosy Department, Faculty of Pharmacy, University of Sadat City, Sadat City 32897, Egypt.

[c]Narcotics, Ergogenics and Poisons Department, Medical Research and Clinical Studies Institute, National Research Centre , Egypt.

***Corresponding author:**

Mailing Address: Pharmaceutical Technology Department, National Research Centre, 33 El-Buhouth Street, Dokki, Cairo, 12622, Egypt.

E-mail: m_mona14@hotmail.com, mm.samra@nrc.sci.eg

Orcid number: 0000-0001-5027-1149

Abstract

This study tackles the development of morin hydrate loaded Phyto-Emulsomes (MH-EMs) using *β*-sitosterol as a 'heart-friendly' alternative to cholesterol for curing leukemia. *β*-sitosterol was isolated from the aerial parts of *C. pallescens* Delile (Compositae). Then, Phyto-Emulsomes were prepared using different ratios of glyceryl monostearate , phospholipon 80H and ß-sitosterol , then, their size, entrapment efficiency, and drug release were evaluated. Among the prepared formulae, MH-EM5 composed of GMS: P80H: SS (2:0.5:0.5) had the highest drug release (RE =82.28±1.96 %) and the smallest particle size (271.7±4.86 nm) with a uniform distribution. MH-EM5 was subjected to characterization including the micro-morphological examination using TEM, thermal analysis, in addition to biological evaluation. The biostability of MH-EM5 in serum and bile salts was proved. The potential cytotoxicity of the free drug, MH-EM5 and its corresponding unmedicated formulation against normal oral epithelial cell and acute monocytic leukemia was studied. The results showed a negligible cytotoxicity in normal cells for all tested samples, while, cancer cell showed a significant decrease in the cell viability for the selected formula (MH-EM5) compared to the corresponding unmedicated formula (EM5) as well as the free drug at different concentrations up to 300 µg/ml. Also, the oral bioavailability study proved the significant increase of all measured pharmacokinetic parameters, after a single oral administration of MH-EM5 compared to the free drug suspension (MH). Regarding these findings, phyto-emulsomes can be considered as a safe and promising nanometric delivery system for the oral administration of morin hydrate due to enhancement of its solubility, oral bioavailability and antitumor efficacy.

Keywords

Morin; emulsomes; leukemia; cytotoxicity; pharmacokinetic

Introduction

Leukemia is a cancer type affecting the developing blood cells of the bone marrow. In 2020, about 60530 cases of leukemia and 23100 deaths have been reported in the USA by the American Cancer Society for Leukemia [1]. Liquid tumors such as leukemia are different from solid tumors and are more complicated because they cannot be removed by surgery. Because conventional treatments are toxic especially with long-term use, shifting towards safer therapeutics is crucial. The construction and development of drug nano-carriers that can be efficient against leukemia is one of the prominent issues in the area of leukemia research [2]. The nanometric drug delivery system can improve drug solubility, enhance bioavailability, prolong blood circulation time, and can also selectively release the drugs at specific sites, and consequently they can ameliorate the therapeutic effect and reduce the systemic toxicity

Many naturally occurring compounds have an anticancer activity by inhibiting cell cycle progression and inducing apoptosis in tumor cells[3]. Morin hydrate is a flavonol mainly found in herbs, red wine and fruits [4] which is s classified as class IV (low solubility and low permeability) according to the Biopharmaceutics Classification System (BCS). It has multiple of biological activities like anti-inflammatory, antioxidant [5], antiproliferative and anticancer [6] . Despite the possession of these beneficial properties, the low aqueous solubility (28.7µg/ml) and poor oral bioavailability remain some of the bioflavonoid's major limitations that restricts its application in the pharmaceutical and medical field[7, 8]. A previous study depicted the drastically low bioavailability of Morin after oral administration of a single dose, and a consequent failure to achieve plasma therapeutic level [9]. To overcome these constraints, various nanoparticulate systems such as niosomes[8] , polymeric nanoparticles[10] , micelles[11] , spray-dried solid dispersions[12] , nanosuspension[13] , and SLNs[3] have been established for the delivery of MH. Also, nanomedicine is a powerful strategy to improve cancer treatment due to the enhanced permeability and retention of nanoscale therapeutics. Nanoencapsulation is one of the methods used to deliver effectively insoluble compounds. Not only does nanoencapsulation improve drug solubility, permeation and bioavailability, but it can also increase drug stability and targeted delivery. However, there has been few research studying the encapsulation of MH in nanovesicles,

therefore an attempt has been made to load the drug into vesicular nano-vectors and evaluate its effect in improving its oral bioavailability.

Vesicular nano-vectors have a multilamellar or unilamellar spheroid structures formed of lipid molecules assembled into bilayers. They are widely investigated as drug carriers for controlled release, drug targeting, or increasing solubility [14]. Also, they are designed to overcome drug related issues such as poor bioavailability, protection from harsh gastric environment, and protection from gastric enzymes that degrade the drug[15]

Emulsomes are developed as novel lipoidal vesicular system composed of lipid cores stabilized by at least one phospholipid layer surrounding the lipid core at the aqueous interface, thereby forming bilayers, which confer stability to the emulsion [16, 17]. Emulsomes (EMs) provide many advantages versus liposomes and lipid carriers. When compared with liposomes and other vesicular systems, they offer some benefits including the avoidance of stability problems such as aggregation, oxidation and susceptibility to hydrolysis. Also, they do not require any co-solvent or surfactant for their preparation and are suitable vehicles for insoluble drugs [18].

On the other side, the main feature of EMs is that the inner fat core is in a liquid crystalline or solid state rather than a fluid oil phase which enables for the entrapment of a higher drug amount. In addition, compared to lipid nanoparticles, they avoid the shortcomings of preparation technique using high pressure such as lipid crystallization, induced drug degradation, gelation and co-existence of several colloidal species are induced [19]. Also, lipid nanoparticles have shown limited controlled release ability because of lipid solidification in phase-separated crystals which precipitate either on the surface of the nanoparticles or in the core [20].

All these properties characterizing EMs can assure improved solubility, cell permeation, bioavailability, and consequently efficacy of insoluble drugs.

Plant sterols (Phytosterols) are structurally related to cholestrerol and are found as fatty acyl conjugates in the cytoplasmic lipid bodies [21]. *β*-sitosterol (C29 24-ethyl cholesterol) is one of the plant sterols which revealed an anti-cancer effect [22]. It has an effect on a variety of disease targets by activating several signaling pathways, implying that it might have a role in the treatment of multifactorial and complex illnesses like cancer [23]. Also, it showed an anti-proliferative and anti-apoptotic effect in human leukemia cell lines via different pathways [24-26]. Although its

therapeutic benefits, *β*-sitosterol has received little attention as a bioactive component due to its low water solubility, limiting its bioavailability; that can be enhanced by nano-encapsulation. In the current study, *β*-sitosterol is extracted, separated and characterized from *Centaurea pallescens*, an annual plant in the Compositae family [27]. As phytosterols are structurally similar to cholestrerol, they can be used as its alternative to decrease the incidence of cardiovascular diseases while using products containing cholesterol [16][28].

This is the first study trying to combine the benefits of the heart-friendly alternative to cholesterol (*ß*-sitosterol) with those of the novel nano-vesicular vector (Emulsomes), to encapsulate the water-insoluble polyphenolic compound of natural source (Morin hydrate) in a trial to present a safe and efficient nano-therapeutic "Phyto-Emulsomes" to combat leukemia. The study comprised the preparation, characterization and in-vitro evaluation of the prepared emulsomes followed by biological evaluations comprising cell biology and pharmacokinetic studies.

2. Materials and methods

2.1. Materials

Morine hydrate (MH) was purchased from Santa Cruz,USA. Phospholipon 80 H (hydrogenated phospholipids from soybean with 80% phosphatidylcholine) (P80H) was kindly gifted from lipoid, Switzerland. Glyceryl monostearate (GMS) and cellulose membrane [molecular weight cut-off (MWCO): 12,000–14,000] were purchased from Sigma-Aldrich Chemical Company (St. Louis, Missouri, USA). All other chemicals and solvents utilized in this research were of analytical grade. The aerial parts of *C. pallescens* (F: Compositae) were collected in April 2020 from El-Orman Garden, Giza, Egypt. The herb was kindly identified by the Taxonomist Mrs. Terase Labib, El-Orman Garden. A voucher sample of *C. pallescens* was kept in the herbarium at the same garden.

2.2. Methods

2.2.1. Extraction and isolation of *β*-sitosterol

The pulverized aerial parts of *C. pallescens* (1 kg) were extracted in ethanol (3 L x 2) at 25 C°. The ethanol extract (100 g) was concentrated, suspended in water, and then fractionated by dichloromethane (5 × 400 mL). The combined fraction (15 g) was subjected to column chromatography packed with silica gel 60 (300 g, 63–200 μm, 5×100 cm) with gradient elution using petroleum ether and ethyl acetate. The eluted fractions (30 mL each) were collected, and monitored by thin layer chromatography (TLC) then for spot visualization, spayed with 10% H_2SO_4 and heated at 100 C°. Three similar fractions eluted with petroleum ether: ethyl acetate (8:1) were combined together then concentrated to crystalize *β*-sitosterol in a pure form (96%).

Test for alcohol

β-Sitosterol was dissolved in dioxane then ceric ammoinium nitrate was added to produce a yellow to reddish color [29].

Spectroscopic analysis

UV-visible spectroscopy, Carbon nuclear magnetic resonance (^{13}C-NMR) and mass (MS) spectroscopy were applied for structural elucidation of the isolated crystals (*β*-sitosterol). The UV-visible spectrum was recorded on a Shimadzu UV-2600 UV-vis spectrophotometer (Tokyo, Japan). The ^{13}C-NMR analysis was performed using $CDCl_3$ as solvent and TMS (tetramethylsilane) as internal standard at 100 MHz on a Bruker AscendTM NMR spectrometer (Billerica, Massachusetts, USA). The mass spectrum was recorded on a JEOL JMS-700 spectrometer (Tokyo, Japan).

2.2.2. Preparation of drug-loaded emulsomes (MH-EMs)

MH-loaded emulsomes (MH-EMs) were prepared by the thin film hydration technique [30, 31]. Briefly, the lipidic components together with the drug (1 mg/ml) are dissolved together in a mixture of chloroform: methanol (1:1), the composition is listed in table 1. Then, the organic solvents were evaporated for 30 minutes using a rotary evaporator (Buchi, Flawil, Switzerland) at 60 °C and a rotation speed of 90 rpm. The dry film was then hydrated with 10 ml of phosphate buffer (pH=6.8) and left for rotation for one hour to allow the vesicles to be formed at normal atmospheric pressure. Finally, the prepared vesicular formulations were stored in tightly closed vials for further assessments. All samples were prepared in triplicates.

2.2.3. Assessment of MH-EMs

2.2.3.1. Determination of the drug entrapment efficiency (EE%)

The prepared EMs' entrapment efficiency was measured indirectly. Samples were centrifuged at 9000 rpm for one hour at 4°C in a cooling centrifuge (Union 32R, Korea). The supernatant was collected, filtered through a millipore membrane filter (0.2µm), and diluted with methanol before being measured at 390 nm with a Shimadzu UV spectrophotometer (2401/PC, Japan). The following equation was used to calculate the entrapment efficiency:

$$EE\% = \frac{Wa - Ws}{Wa} \times 100$$

Where Wa and Ws, are weights of drug added into the preparation and weight of the drug in the supernatant, respectively [32].

2.2.3.2. Vesicle size analysis and polydispersity index (PDI)

Photon correlation spectroscopy was used to determine the size and PDI of nanovesicles using a Zetasizer (Malvern Instrument, Worcestershire, UK) at a fixed angle of 90° at 25° C. Before measuring particle size, samples were diluted with distilled water (1:10) to achieve a suitable scattering intensity.

2.2.3.3. Zeta potential measurement

The particle charge was quantified as zeta potential (ZP) using a Zetasizer (Malvern Instrument, Worcestershire, UK) at 25ºC. Before measuring, each sample was diluted with distilled water (1:10).

2.2.4. In-vitro release studies of MH-loaded EMs

The dialysis bag diffusion technique was used to study the drug release from the prepared MH-loaded EMs compared to that of the drug aqueous suspension containing an equivalent amount of the drug (1 mg) using cellulose acetate dialysis bags (molecular weight cutoff 12,000-14,000). The dialysis bag (donor compartment) was immersed in the receptor compartment containing 100 ml phosphate buffer with different pH values (6.8 and 7.4) with 20% methyl alcohol to maintain sink condition [33], stirred at 100 rpm and maintained at 37±0.5ºC. At fixed time intervals (0.5, 1,

2, 3, 4, and 5 h), samples (2 ml) were withdrawn from the receptor compartment and replaced with the same volume of fresh release medium to keep a constant volume. The percentage of MH released was measured spectrophotometrically at 390 nm. Results were carried out in triplicate and the results were expressed as the mean values ±S.D. The release efficiency was calculated using the trapezoidal rule and the release kinetics were studied to find the best fitting model.

* Statistical analysis was performed using one-way analysis of variance (one-way ANOVA) and Least Significant Difference test by SPSS® software (version 16, SPSS Inc., Chicago, USA). Differences were significant when $p<0.05$.

2.2.5. Characterization of the selected MH-loaded EMs

Depending on the results previously obtained from the entrapment efficiency, vesicle size, PDI and the in-vitro drug release; a selected MH-loaded emulsomes formulation was exposed to more investigations.

2.2.5.1. Transmission electron microscopy (TEM)

The micro-morphological examination of the selected drug-loaded phyto-emulsomes was done by a TEM (JEOL JEM1230, Tokyo, Japan) operating at an accelerating voltage of 80 kV. The sample was deposited on the surface of a carbon-coated copper grid and left for 1 min, and then micrographs were taken at suitable magnification power at room temperature.

2.2.5.2. Differential scanning calorimetry (DSC) of MH-loaded EMs

The selected MH-loaded emulsomes was subjected to lyophilisation (Novalyphe-NL 500; Savant Instruments Corp., Hicksville, NY, USA) prior to DSC analysis. The thermal characteristics of MH, *ß*-sitosterol (SS), GMS, (P80H) and the selected MH- loaded EMs were determined by differential scanning calorimetry DSC131 evo (SETARAM Inc., France). The test was carried out at temperatures ranging from 25°C to 350°C, with a heating rate of 10°C/min. The sample was first weighted in an aluminium crucible before being introduced to the DSC. The thermogram data was analyzed using (CALISTO Data processing software v.149).

2.2.5.3 Study of MH-loaded EMs serum stability

The effect of serum protein on the stability of the selected MH-loaded emulsomes was investigated using fetal bovine serum (FBS) incubated at 37°C to mimic physiological media[34]. In brief, sample was mixed with FBS in a ratio of 1:10 and the average particle size was measured at various incubation times (0, 1, 2, 4 & 24 h).

2.2.5.4. Study of MH-loaded EMs stability in bile salt solution

The stability of the selected MH-EMs was evaluated according to the turbidity method previously performed by Varshosaz et al., [35]. Briefly, the formulation was incubated in different concentrations of sodium deoxycholate solutions (0-20 mM in PBS, pH 7.4) at 37°C for 60 min. Turbidity of the solutions after incubation was measured spectrophotometrically at 400 nm (Shimadzu UV 2401/PC, Japan) and the turbidity percent was calculated according to the following equation[36]:

$$\boldsymbol{Turbidity}\ \% = \frac{\mathbf{a}}{\mathbf{b}}\ \boldsymbol{x}\ \mathbf{100}$$

where a is the absorbance of MH-EMs incubated in bile salt solution and b is the absorbance of MH-EMs incubated in PBS pH 7.4 .

2.2.6. Cell viability assay

2.2.6.1. Cell culture

Oral epithelial cell (OEC) and Acute monocytic leukemia (AML) cell line (Kasumi-1) were obtained from Nawah Scientific Inc., (Mokatam, Cairo, Egypt). Cells were cultured in Roswell Park Memorial Institute Medium (RPMI) supplemented with 100 units/mL penicillin ,100 mg/mL streptomycin , and 10% heat-inactivated foetal bovine serum at 37 °C in a humidified, 5% (v/v) CO_2 atmosphere.

2.2.6.2. Cytotoxicity assay

The cell viability was determined using the water soluble tetrazolium salt (WST-1) assay and the Abcam® kit (ab155902 WST-1 Cell Proliferation Reagent). In 96-well plates, samples of 50 µL cell suspension ($3x10^3$ cells) were seeded and incubated in complete media for 24 hr. Cells were then treated with 50 µL media containing an equivalent weight of the free drug (MH) or MH-

loaded EM5 (MH-EM5) or the corresponding unmedicated formula (EM5) at various concentrations (0.03, 0.3, 3, 30, and 300 µg/ml). Cells were treated with 10 µL WST-1 reagent after 48 hr of exposure, and absorbance was measured at 450 nm after 1 hour using a BMG LABTECH®- FLUO star Omega microplate reader (Allmendgrün,Ortenberg).

2.2.7. Pharmacokinetic study

Animals

Twelve adult male Wistar rats weighing 200-250 g were obtained from the National Research Centre's Animal House Colony in Giza, Egypt, and housed in polypropylene cages in an environmentally controlled clean air room with a temperature of 25±1°C, an alternating 12 h light/12 h dark cycle, a relative humidity of 60±5%, and free access to tap water and a standard rodent chow (Wadi El Kabda Co., Cairo, Egypt). The rats were given two weeks to adjust to their new surroundings before the experiment began. The study protocol was approved by the Ethical Committee of the Medical Research of the National Research Centre, Egypt, and followed the ethical guidelines for animal experiments.

Instrumentation and chromatographic conditions

MH was analyzed in plasma using RP-HPLC using an UHPLC system (Ultimate 3000, Thermo Inc, USA). Separation was performed on a Zorbax XDB C18 reversed-phase column (15 × 4.6 mm, 5 µm pore size; Agilent, USA) using a mixture of methanol/1 % acetic acid in water as the mobile phase in 80:20 ratio. The flow rate and retention time were 1 ml min−1 and 2.26 min respectively. Detection was performed at 270 nm [37].

Pharmacokinetic studies

The rats were divided into two groups of six animals each. The first group received an oral single dose of MH suspension (10 mg/Kg) [38], while the second group received an equivalent single oral dose of MH- EM5. Diethyl ether was used to anaesthetize the rats before blood samples (0.5 ml) were taken from the retro-orbital plexus at 1, 2, 4, 5, 7, and 24 hr and placed in EDTA-coated micro centrifuge tubes. They were then centrifuged (5000 rpm for 15 min.), and the plasma was decanted and stored in a deep freezer (-20 °C) until analysis, plasma (400 µl) was deproteinized with double volume methanol/acetonitrile (1:1), and then centrifuged (10,000 rpm for 10 min.).

The supernatant layer was filtered using membrane syringe filters (0.45 µm pore size) before being injected into the HPLC column in 50 µl increments.

Pharmacokinetics and statistical analysis

The serum concentration profiles obtained after oral administration of free MH and MH-loaded EM were plotted and, the pharmacokinetic parameters were calculated using a non-compartmental approach (table 4). PK Solver (version 2.0) was used to analyze the data. The data were presented as mean ± standard errors (SE). The unpaired t test was used to determine group differences (Graph Pad Prism 7 software).

3. Results and discussion

3.1. Identification of the compound isolated from *C. pallescens*

The compound was isolated (white crystalline needles) with positive test for alcohols [29], λmax at 220 nm and parent mass peak at *m/z* 414 [M]+ indicating the molecular formula $C_{29}H_{50}O$. The ^{13}C-NMR (100 MHz, $CDCl_3$) data was characterized by two signals at 142.38 and 121.03 ppm ascribed to alkene double bonds at C-5 and C-6, respectively. In addition, the angular methyl carbon atoms were detected at 28.26 and 19.04 ppm credited to C-16 and C-19, respectively. Furthermore, a signal at 74.63 ppm was ascribed to C-3 attached to a hydroxyl group. The spectrum revealed 29 carbon signals in total including 6 methyls, 9 methines, 3 quaternary carbons and 11 methylene groups and the compound was identified as *β*-sitosterol by comparison to previous reported data [39, 40].

3.2. Characterization of MH-loaded emulsomes

The results of the MH-EMs entrapment efficiency, size distribution and zeta potential for the prepared formulations are illustrated in table 2. Entrapment efficiency is a critical tool for estimating drug retention in the nanovesicles in order to deliver a sufficient amount of the drug [41].All the prepared formulae had a high entrapment efficiency ranging between 78.45±0.80 and 80.64±1.21%. As explained above, emulsomes are nanovesicles composed of lipid cores surrounded by a phospholipid sheath at the aqueous interface, forming a bilayered structure, hence stabilizing the emulsion. Therefore, the recorded high encapsulation efficiency can be expected due to the lipophilicity of the drug under study.

Results of the particle size analysis for the MH-EMs and their corresponding PDI values listed in table 2 reveal that all the prepared formulae were in the nanometric range falling between 271.7±4.86 and 645.3±9.12 nm**.** It is clear that vesicles containing ß-sitosterol (SS) exhibited smaller particle size compared to the corresponding vesicles lacking SS (MH-EM1 *vs* MH-EM4, MH-EM2 *vs* MH-EM5 and MH-EM3 *vs* MH-EM6). This finding can be explained by the alteration of the surface tension of the prepared vesicles accompanying the incorporation of SS during formulation. SS cause increase in the hydrophilic nature of the lipid bilayer associated with a decrease in the surface tension of the prepared MH-loaded emulsomes lead to an increase of the membrane surface, and as a result, the particle size of the vesicular dispersions was shifted to smaller size distributions[42]. On the other hand, it had been recorded that using hydrogenated phospholipids with a high percentage of phosphatidylcholine such as P80H yielded large vesicles [31, 43], therefore emulsomes with higher proportions of P80H had higher particle sizes (MH-EM3 > MH-EM1> MH-EM2) and (MH-EM6 > MH-EM4> MH-EM5). Also, the replacement of a part of P80H by SS resulted in the decrease of particle size (MH-EM1 *vs* MH-EM4, MH-EM2 *vs* MH-EM5 and MH-EM3 *vs* MH-EM6).

The polydispersity index was used to indicate the uniformity of vesicular size within the formulation. High PDI values identify a heterogeneous population with a high aggregation tendency which affects the stability of the preparation, while small PDI values reveal homogenous monodisperse size distribution [44, 45] [46]. As demonstrated in table 2, all the PDI values for the designed MH-loaded EMs exhibited values less than 0.5 which reveals homogeneity of size distribution [47].

All the prepared MH-loaded emulsomes demonstrate a negatively charged surface with ZP values ranging from -33.5 to -37.5 (Table 2). It is well recognized that surface charge values that are more positive than (+30 mV) or more negative than (-30 mV) can provide a good physical stability by generating electrostatic repulsion between the vesicles, which prevents vesicle aggregation or coalescence [7, 48].

3.3. In-vitro release studies of MH-loaded emulsomes

The release profiles of different MH-loaded emulsomes as well as MH suspension are illustrated in Figure 1 (a &b). The drug release followed the same behavior at both pH (6.8 and 7.4) and there

was no significant difference between the amount of drug released at the tested time intervals, this may be due to that the pKa of the drug (3.46) [49] is far below the used pH values . The faster drug release from the emulsomes is clear. Data listed in table 3 (a &b) clearly shows a significant increase of drug release from the prepared nanoformulae compared to the drug suspension as detected from the values of the release efficiency ($p<0.05$). This is expected due to the solublization and nano-encapsulation of the hydrophobic drug within the vesicular structure. Another factor that contributes to the faster drug release from the tested formulations versus the free drug is the use of P80H which is a natural emulsifier that allows hydration of the emulsomes by the dissolution medium and formation of elution channels within the vesicles structure [50] allowing for the drug to escape out. The enhancement ratio is calculated as the release efficiency of the different formulae relative to that of the drug suspension, the enhancement ranged from 2.21 to 5.87 folds. The results can be correlated with those of the particle size, with the nanovesicles of smaller size attaining a faster drug release due to the larger surface area exposed to the external release medium. All the MH-loaded emulsomes show biphasic release pattern, with an initial drug fast release phase followed by a slower phase. The initial burst release is caused by the release of the drug adsorbed on the vesicles surface to the external medium, while the sustained release can be the result of the release of the drug from the inner lipid core [51, 52]. As predicted from the results, the emulsomes prepared with SS attained higher release compared to their corresponding nanovesicles prepared with P80H only (MH-EM4>MH-EM1, MH-EM5>MH-EM2 and MH-EM6>MH-EM3). This can be explained by the smaller, less ordered, more fluid structure for the prepared nanovesicles resulting from the decrease of vesicles surface tension caused by the presence of SS [42].

All the emulsomes under study followed a diffusion-dependent release model (as listed in table 3 a&b) which is the common one for vesicular systems [53, 54].

Among the prepared formulae, MH-EM5 composed of GMS: P80H: SS (2:0.5:0.5) had the faster drug release reaching a complete drug release within 5 h, it attained the highest release enhancement ratio (about 6 fold). Also, it had the smallest particle size and showed a uniform size distribution; hence this MH-loaded phyto-emulsome was selected as the most suitable formula and was subjected to further investigations including the morphological examination, thermal analysis, in-vitro and in-vivo biological evaluation.

3.3. Characterization of the selected MH-loaded phyto-emulsomes

3.3.1. Transmission electron microscopy

TEM analysis is a useful tool for studying the morphological properties of nanovesicles. Figure 2(a), illustrates the micrograph of the selected phyto-emulsomes (MH-EM5), where the vesicles appeared to be almost spherical, uniform and non-aggregating with a dense inner core. The figure clearly shows that the diameter of the vesicles observed in the micrograph was in the nano-range and agreed with the Zetasizer measurement.

3.3.2. Differential scanning calorimetry

The thermal analysis of MH, GMS, P 80H, SS and MH-EM5 are presented in Fig. 2 (b). MH exhibits a sharp endothermic melting peak at 287.47°C as a result of drug melting, confirming its crystallinity [55]. Similarly, the DSC thermogram of GMS and P80H display endothermic peaks at 62.4 ºC and 83 ºC, respectively, corresponding to their melting temperature [56, 57]. As well, the thermogram of SS shows an endothermic peak at 92°C. In contrast, the thermogram of the selected preparation (MH-EM5) revealed the absence of all the characteristic peaks belonging to MH, GMS and SS, indicating that MH was encapsulated within the formulated nano-vesicular structure and highlighting the amorphous nature of the drug after its incorporation into the nano-vesicles.

3.3.3. MH-EMs serum stability

Figure 3(a) demonstrates that there was no significant difference in the particle size of the samples measured at different time intervals, all ranged between 310.5±10 and 322±9 nm, this can indicate the stability of the prepared nano-vesicles in serum. It is well known that the incorporation of a certain drug in a lipid bilayer structure may be a good strategy to impart stability to nanoparticles in the biological fluids by forming a coating layer mimicking the cell membrane and producing a stealth effect [58].

3.3.4. MH-EMs stability in bile salt solution

Turbidimetry has been the most frequently used technique for investigating surfactant (bile salts) interaction with vesicles, particularly important for an oral dosage form design [35].As seen in figure 3(b), no abrupt change was observed in turbidity percent at the all the studied bile salts concentrations indicating the resistance to bile salt lysis and the biostability of the tested nano-vesicles. It is here to mention that it was previously reported that the lipid bilayer structure forms a coat providing high stability in salt solutions [59, 60].

3.6. Biological studies

3.6.1. Cell viability in normal cells

The cytotoxicity of the free drug (MH) was compared to that of the selected drug-loaded emulsomes (MH-EM5) and its corresponding unmedicated formula (EM5), at different concentrations (0.03, 0.3, 3, 30, and 300 g/ml), in normal cells. All the samples displayed negligible cytotoxic effect on human normal OEC in all tested concentrations (Figs 4&5), the viability was higher than 90% in all cases proving their safety and cytocompatibility.

3.6.2. Cell viability in cancer cells

The cytotoxicity of the free drug (MH) was compared to that of the selected drug-loaded emulsomes (MH-EM5) and its corresponding unmedicated formula (EM5), at different concentrations (0.03, 0.3, 3, 30, and 300 g/ml), in cancer cells. Figures 6 and 7 clearly depict a significant and concentration-dependent decrease in cell viability of AML cell lines after application of the tested samples. The results show a significant decrease in the cell viability in the case of MH-EM5 formula compared to the unmedicated one as well as the free MH at tested concentrations (3µg/mL up to 300µg/mL) ($p<0.05$), the cytotoxic effect of the tested samples was found to be in that order MH-EM5 > EM5 > MH (Fig.6). The weak effect of the drug suspension (MH) was expected due to its poor solubility and permeability. The optical microscopy images (Fig. 7) also show the morphology and distribution of cells in comparison to the control after 48 hours of treatment with the different concentrations of the tested samples, it can be detected that the number of cells decreased, and the remaining cells had a reduced size with noticeable cell shrinkage. The significantly higher efficacy of the MH-EM5 compared to the free MH may be attributed to drug encapsulation in the prepared emulsomes (MH-EM5), which resulted in

solubilization of the poorly soluble drug under study and improved its penetration and uptake into the cells[61], these caused a higher cellular damage and cytotoxicity and augmented the anti-proliferative effect of the drug. In the same context. a previous study has discussed the improved increased cellular uptake of morin by nano-emulsification [62].

Also, the use of ß-sitosterol for the preparation of the studied formula enhanced its effect due to its cytotoxic and apoptotic properties [63, 64], which can explain the anti-regenerative effect of the tested unmedicated formula. The pathogenesis of leukemia is complicated; it is not possible to obtain an ideal treatment using a single effective component. Therefore, multiple effective agent with different mechanisms of action can provide a synergistic effect and a better treatment can be achieved.

The negligible cytotoxicity in normal cells and the high cytotoxic effect in cancer cells can prove the safety and selectivity of the tested nano-formula.

3.6.2. Pharmacokinetic study

The plasma profile of the drug under study after oral administration of a single oral dose of the crude drug suspension (MH) or the prepared drug-loaded emulsomes (MH-EM5) is shown in figure 8. It is clear that in the case of the drug suspension the maximum plasma concentration was attained at about 1 h followed by a continuous abrupt fall in drug level till reaching an almost complete clearance at 7 h. While, in the case of the formulated MH-EM5, the peak drug level was attained at about 2 h, then, there was a gradual decrease of drug level till 24 hr. The calculated pharmacokinetic parameters corresponding to MH and MH-EM5 are listed in table 4, a significant improvement ($p<0.5$) of all parameters can be clearly seen. Oral administration of MH-loaded EM resulted in a significant increase in the peak plasma MH concentration (C_{max}) to about 1.25 fold. Extent of bioavailability, expressed as AUC, increased 3-fold. Notably, AUMC was increased in group receiving MH-loaded EM to about 9 fold. Time to peak concentration (t_{max}) was prolonged to 2 hr. Mean residence time (MRT) increased more than 2-fold. Elimination rate constant (λz) and clearance (CL/F) were decreased in MH-loaded EM group relative to MH group.

The pharmacokinetic analysis revealed that the newly developed MH- EM5 provided higher bioavailability, in terms of increased AUC and AUMC. The increased solubility and absorption was evident in the higher C_{max} observed after administering MH-EM5. Being nanosized, the prepared EM exhibits higher drug solubility and absorption by facilitating cell membrane

penetration and resulting in a more efficient drug delivery [65, 66]. In addition, the presence of phospholipids (P80H) and ß-sitosterol (SS) in the composition of the prepared nanoparticles can enhance its absorption as they are amphiphilic molecules which are an integral part of the living cell and can fuse with the cell membrane and deliver the drug into the cell [67, 68]. Vesicular structures are highly ordered with one or more concentric lipid bilayer consisted of amphiphilic ingredients and water, they which can prolong drug existence, target delivery, retard elimination, and therefore enhance drug bioavailability [69]. Vesicles rich in cholesterol and phospholipids have enhanced the effect of many drugs of plant origin [70].

It was also proved in a previous study that phospholipid-Morin complex protected the drug from intestinal degradation and increased duodenum-specific intestinal drug permeability [71], another study discussed the possible mechanisms of the increased cellular uptake by emulsification of morin [62].

Besides that, the use of surface active agents enhance drug permeability across cell membranes by decreasing plasma membrane transporter P-glycoprotein (P-gp), and increasing mucosal adhesion resulting in the increment of bioavailability [72]. Also, drug encapsulation can protect it from first-pass metabolism [73]. Based on the above, we can therefore confirm that our suggested formula significantly improved drug oral bioavailability.

Conclusion

The key factor for fighting leukemia is to seek novel combined drug delivery systems that can improve drug biological performance. In this study, Morin hydrate loaded phyto-emulsomes (MH-EMs) were successfully prepared using *β*-sitosterol as a 'heart-friendly' alternative to cholesterol. The MH-loaded EM showed a significant increase in drug release. The selected formula (MH-EM5) was characterized using TEM and DSC, then, biologically evaluated. The cell biology studies showed a significant increase in cytotoxicity for the tested formula compared to the corresponding unmedicated formula as well as the free drug, and also proved the selectivity against cancer cells. Moreover, the oral bioavailability study proved the significant increase of all measured pharmacokinetic parameters, after single oral administration, of MH-EM5 compared to

the free MH. We can therefore claim that the prepared phyto-emulsomes can be considered as a promising nanovector for the oral administration of MH, which enhanced its solubility, oral bioavailability and antitumor efficacy.

Disclosure statement

Authors declare no conflict of interest.

References

[1] Z. Wan, R. Sun, P. Moharil, J. Chen, Y. Liu, X. Song*, et al.*, "Research advances in nanomedicine, immunotherapy, and combination therapy for leukemia," *Journal of Leukocyte Biology,* vol. 109, pp. 425-436, 2021.

[2] J. Shen, Z. Lu, J. Wang, T. Zhang, J. Yang, Y. Li*, et al.*, "Advances of Nanoparticles for Leukemia Treatment," *ACS Biomaterials Science & Engineering,* vol. 6, pp. 6478-6489, 2020/12/14 2020.

[3] S. Karamchedu, L. Tunki, H. Kulhari, and D. Pooja, "Morin hydrate loaded solid lipid nanoparticles: Characterization, stability, anticancer activity, and bioavailability," *Chem Phys Lipids,* vol. 233, p. 104988, Nov 2020.

[4] J.-Y. Lee, S.-O. Moon, Y.-J. Kwon, S.-J. Rhee, H.-R. Park, and S.-W. Choi, "Identification and quantification of anthocyanins and flavonoids in mulberry (Morus sp.) cultivars," *Food Science and Biotechnology,* vol. 13, pp. 176-184, 2004.

[5] Y. Hanasaki, S. Ogawa, and S. Fukui, "The correlation between active oxygens scavenging and antioxidative effects of flavonoids," *Free Radical Biology and Medicine,* vol. 16, pp. 845-850, 1994.

[6] H.-M. Kuo, L.-S. Chang, Y.-L. Lin, H.-F. Lu, J.-S. Yang, J.-H. Lee*, et al.*, "Morin inhibits the growth of human leukemia HL-60 cells via cell cycle arrest and induction of apoptosis through mitochondria dependent pathway," *Anticancer research,* vol. 27, pp. 395-405, 2007.

[7] A. K. Jangid, D. Pooja, and H. Kulhari, "Determination of solubility, stability and degradation kinetics of morin hydrate in physiological solutions," *RSC Advances,* vol. 8, pp. 28836-28842, 2018.

[8] A. Y. Waddad, S. Abbad, F. Yu, W. L. Munyendo, J. Wang, H. Lv*, et al.*, "Formulation, characterization and pharmacokinetics of Morin hydrate niosomes prepared from various non-ionic surfactants," *Int J Pharm,* vol. 456, pp. 446-58, Nov 18 2013.

[9] Y. Hou, P. Chao, H. Ho, C. Wen, and S. Hsiu, "Profound difference in pharmacokinetics between morin and its isomer quercetin in rats," *Journal of pharmacy and pharmacology,* vol. 55, pp. 199-203, 2003.

[10] S. Abbad, C. Wang, A. Y. Waddad, H. Lv, and J. Zhou, "Preparation, in vitro and in vivo evaluation of polymeric nanoparticles based on hyaluronic acid-poly(butyl cyanoacrylate) and D-alpha-tocopheryl polyethylene glycol 1000 succinate for tumor-targeted delivery of morin hydrate," *Int J Nanomedicine,* vol. 10, pp. 305-20, 2015.

[11] A. K. Jangid, H. Agraval, N. Gupta, U. C. S. Yadav, R. Sistla, D. Pooja*, et al.*, "Designing of fatty acid-surfactant conjugate based nanomicelles of morin hydrate for simultaneously enhancing anticancer activity and oral bioavailability," *Colloids Surf B Biointerfaces,* vol. 175, pp. 202-211, Mar 1 2019.

[12] A. D. Kulkarni and V. S. Belgamwar, "Influence of novel carrier Soluplus® on aqueous stability, oral bioavailability, and anticancer activity of Morin hydrate," *Drying Technology,* vol. 37, pp. 1143-1161, 2019/07/04 2019.

[13] A. K. Jangid, H. Agraval, N. Gupta, P. Jain, U. C. S. Yadav, D. Pooja*, et al.*, "Amorphous nano morin outperforms native molecule in anticancer activity and oral bioavailability," *Drug Dev Ind Pharm,* vol. 46, pp. 1123-1132, Jul 2020.

[14] I. P. Kaur, A. Garg, A. K. Singla, and D. Aggarwal, "Vesicular systems in ocular drug delivery: an overview," *Int J Pharm,* vol. 269, pp. 1-14, 2004.

[15] B. Gill, J. Singh, V. Sharma, and S. L. Kumar, "Emulsomes: An emerging vesicular drug delivery system," *Asian Journal of Pharmaceutics,* vol. 6, p. 87, 04/01 2012.

[16] B. Gill, J. Singh, V. Sharma, and S. H. Kumar, "Emulsomes: An emerging vesicular drug delivery system," *Asian Journal of Pharmaceutics (AJP): Free full text articles from Asian J Pharm,* vol. 6, 2014.

[17] A. Pal, S. Gupta, A. Jaiswal, A. Dube, and S. P. Vyas, "Development and evaluation of tripalmitin emulsomes for the treatment of experimental visceral leishmaniasis," *J Liposome Res,* vol. 22, pp. 62-71, 2012.

[18] G. M. El-Zaafarany, M. E. Soliman, S. Mansour, and G. A. Awad, "Identifying lipidic emulsomes for improved oxcarbazepine brain targeting: In vitro and rat in vivo studies," *Int J Pharm,* vol. 503, pp. 127-140, 2016.

[19] A. Elgart, I. Cherniakov, Y. Aldouby, A. J. Domb, and A. Hoffman, "Lipospheres and pro-nano lipospheres for delivery of poorly water soluble compounds," *Chemistry and physics of lipids,* vol. 165, pp. 438-453, 2012.

[20] M. Garcia-Fuentes, M. J. Alonso, and D. Torres, "Design and characterization of a new drug nanocarrier made from solid–liquid lipid mixtures," *J Colloid Interface Sci,* vol. 285, pp. 590-598, 2005.

[21] R. A. Moreau, L. Nyström, B. D. Whitaker, J. K. Winkler-Moser, D. J. Baer, S. K. Gebauer*, et al.*, "Phytosterols and their derivatives: Structural diversity, distribution, metabolism, analysis, and health-promoting uses," *Progress in Lipid Research,* vol. 70, pp. 35-61, 2018.

[22] S. Babu and S. Jayaraman, "An update on β-sitosterol: a potential herbal nutraceutical for diabetic management," *Biomedicine & Pharmacotherapy,* vol. 131, p. 110702, 2020.

[23] L. Novotny, M. Abdel-Hamid, and L. Hunakova, "Anticancer potential of β-sitosterol," *Int J Clin Pharmacol Pharmacother,* vol. 2, pp. 2-4, 2017.

[24] C. Park, D.-O. Moon, C.-H. Rhu, B. T. Choi, W. H. Lee, G.-Y. Kim*, et al.*, "β-Sitosterol induces anti-proliferation and apoptosis in human leukemic U937 cells through activation of caspase-3 and induction of Bax/Bcl-2 ratio," *Biological and Pharmaceutical Bulletin,* vol. 30, pp. 1317-1323, 2007.

[25] M. S. Bin Sayeed and S. S. Ameen, "Beta-sitosterol: a promising but orphan nutraceutical to fight against cancer," *Nutrition and cancer,* vol. 67, pp. 1216-1222, 2015.

[26] T. Woyengo, V. Ramprasath, and P. Jones, "Anticancer effects of phytosterols," *European journal of clinical nutrition,* vol. 63, pp. 813-820, 2009.

[27] A. M. Ahmed, S. Eisa, I. El-Shamey, A. Mohamed, and S. Hussin, "A study on the flora of El-Qantara Sharq in North Sinai, Egypt," *Annals of Agricultural Sciences,* vol. 60, pp. 169-182, 2015.

[28] J. E. Hokanson and M. A. Austin, "Plasma triglyceride level is a risk factor for cardiovascular disease independent of high-density lipoprotein cholesterol level: a metaanalysis of population-based prospective studies," *Journal of cardiovascular risk,* vol. 3, pp. 213-219, 1996.

[29] G. Angajala and R. Subashini, "Evaluation of larvicidal potential of β-sitosterol isolated from indigenous Aegle marmelos Correa crude leaf extracts against blood feeding parasites and its binding affinity studies towards sterol carrier protein," *Biocatalysis and agricultural biotechnology,* vol. 16, pp. 586-593, 2018.

[30] A. D. Bangham, M. M. Standish, and J. C. Watkins, "Diffusion of univalent ions across the lamellae of swollen phospholipids," *J Mol Biol,* vol. 13, pp. 238-52, Aug 1965.

[31] M. M. AbouSamra, A. H. Salama, G. E. A. Awad, and S. S. Mansy, "Formulation and Evaluation of Novel Hybridized Nanovesicles for Enhancing Buccal Delivery of Ciclopirox Olamine," *AAPS PharmSciTech,* vol. 21, p. 283, Oct 13 2020.

[32] E. B. Souto, W. Mehnert, and R. H. Muller, "Polymorphic behaviour of Compritol888 ATO as bulk lipid and as SLN and NLC," *J Microencapsul,* vol. 23, pp. 417-33, Jun 2006.

[33] R. Kamel and M. Basha, "Preparation and in vitro evaluation of rutin nanostructured liquisolid delivery system," *Bulletin of Faculty of Pharmacy,* vol. 51, pp. 261-272, 2013.

[34] H. Katas, Z. Hussain, and a. S. A. Awang, "Bovine Serum Albumin-Loaded Chitosan/Dextran Nanoparticles: Preparation and Evaluation of Ex Vivo Colloidal Stability in Serum," *Journal of Nanomaterials,* 2013.

[35] J. Varshosaz, A. Pardakhty, V. I. Hajhashemi, and A. R. Najafabadi, "Development and physical characterization of sorbitan monoester niosomes for insulin oral delivery," *Drug Deliv,* vol. 10, pp. 251-62, Oct-Dec 2003.

[36] Z. Sezgin-Bayindir, A. Onay-Besikci, N. Vural, and N. Yuksel, "Niosomes encapsulating paclitaxel for oral bioavailability enhancement: preparation, characterization, pharmacokinetics and biodistribution," *J Microencapsul,* vol. 30, pp. 796-804, 2013.

[37] F. Darvishnejad, J. B. Raoof, and M. Ghani, "Thin film microextraction based on Co3O4@ GO-Nylon-6 polymeric membrane to extract morin and quercetin and determining them through high performance liquid chromatography-ultraviolet detection," *Microchemical Journal,* vol. 170, p. 106684, 2021.

[38] Y. A. Choi, Y. H. Yoon, K. Choi, M. Kwon, S. H. Goo, J.-S. Cha*, et al.*, "Enhanced oral bioavailability of morin administered in mixed micelle formulation with PluronicF127 and Tween80 in rats," *Biological and Pharmaceutical Bulletin,* vol. 38, pp. 208-217, 2015.

[39] M. M. Ododo, M. K. Choudhury, and A. H. Dekebo, "Structure elucidation of β-sitosterol with antibacterial activity from the root bark of Malva parviflora," *SpringerPlus,* vol. 5, pp. 1-11, 2016.

[40] K. P. Manoharan, T. K. H. Benny, and D. Yang, "Cycloartane type triterpenoids from the rhizomes of Polygonum bistorta," *Phytochemistry,* vol. 66, pp. 2304-2308, 2005.

[41] J. Y. Fang, S. Y. Yu, P. C. Wu, Y. B. Huang, and Y. H. Tsai, "In vitro skin permeation of estradiol from various proniosome formulations," *Int J Pharm,* vol. 215, pp. 91-9, Mar 14 2001.

[42] E. Farkas, R. Schubert, and R. Zelko, "Effect of beta-sitosterol on the characteristics of vesicular gels containing chlorhexidine," *Int J Pharm,* vol. 278, pp. 63-70, Jun 18 2004.

[43] M. M. AbouSamra and A. H. Salama, "Enhancement of the topical tolnaftate delivery for the treatment of tinea pedis via provesicular gel systems," *Journal of liposome research,* vol. 27, pp. 324-334, 2017.

[44] H. S. Helmy, A. E. El-Sahar, R. H. Sayed, R. N. Shamma, A. H. Salama, and E. M. Elbaz, "Therapeutic effects of lornoxicam-loaded nanomicellar formula in experimental models of rheumatoid arthritis," *International journal of nanomedicine,* vol. 12, pp. 7015–7023, 2017.

[45] A. H. Salama, A. A. Abdelkhalek, and N. A. Elkasabgy, "Etoricoxib-loaded bio-adhesive hybridized polylactic acid-based nanoparticles as an intra-articular injection for the treatment of osteoarthritis," *International Journal of Pharmaceutics,* vol. 578, 2020.

[46] M. J. Masarudin, S. M. Cutts, B. J. Evison, D. R. Phillips, and P. J. Pigram, "Factors determining the stability, size distribution, and cellular accumulation of small, monodisperse chitosan nanoparticles as candidate vectors for anticancer drug delivery: application to the passive encapsulation of [14C]-doxorubicin," *Nanotechnology, science and applications,* vol. 8, pp. 67-80, 2015.

[47] V. Centis and P. Vermette, "Physico-chemical properties and cytotoxicity assessment of PEG-modified liposomes containing human hemoglobin," *Colloids Surf B Biointerfaces,* vol. 65, pp. 239-46, Sep 1 2008.

[48] D. Hanaor, M. Michelazzi, C. Leonelli, and C. C. Sorrell, "The effects of carboxylic acids on the aqueous dispersion and electrophoretic deposition of ZrO 2," *Journal of the European Ceramic Society,* vol. 32, pp. 235-244, 2012.

[49] N. Arshad, N. K. Janjua, A. Y. Khan, A. Yaqub, T. Burkholz, and C. Jacob, "Natural flavonoids interact with dinitrobenzene system in aprotic media: an electrochemical probing," *Natural Product Communications,* vol. 7, p. 1934578X1200700309, 2012.

[50] Vemuri S, Yu CD, deGroot JS, and R. N., "In vitro interaction of sized and unsized liposome vesicles with high density lipoproteins.," *Drug Dev Ind Pharm,* vol. 16, pp. 1579–84, 1990.

[51] M. Hasan, K. Elkhoury, C. J. F. Kahn, E. Arab-Tehrany, and M. Linder, "Preparation, Characterization, and Release Kinetics of Chitosan-Coated Nanoliposomes Encapsulating Curcumin in Simulated Environments," *Molecules,* vol. 24, May 27 2019.

[52] A. M. Mohsen, M. M. AbouSamra, and S. A. ElShebiney, "Enhanced oral bioavailability and sustained delivery of glimepiride via niosomal encapsulation: in-vitro characterization and in-vivo evaluation," *Drug Dev Ind Pharm,* vol. 43, pp. 1254-1264, Aug 2017.

[53] R. Kamel, M. Basha, and S. H. Abd El-Alim, "Development of a novel vesicular system using a binary mixture of sorbitan monostearate and polyethylene glycol fatty acid esters for rectal delivery of rutin," *J Liposome Res,* vol. 23, pp. 28–36, Oct 19 2013.

[54] M. C. Gohel, M. K. Panchal, and V. V. Jogani, "Novel mathematical method for quantitative expression of deviation from the Higuchi model," *AAPS PharmSciTech,* vol. 1, pp. 43-48, 2000.

[55] S. Mutalik, P. Shetty, V. Venuvanka, H. Jagani, C. Gejjalagere Honnappa, U. Nayak*, et al.*, "Development and evaluation of sunscreen creams containing morin-encapsulated nanoparticles for enhanced UV radiation protection and antioxidant activity," *International Journal of Nanomedicine,* vol. 10, p. 6477, 10/01 2015.

[56] H. Raina, S. Kaur, and A. B. Jindal, "Development of efavirenz loaded solid lipid nanoparticles: Risk assessment, quality-by-design (QbD) based optimisation and physicochemical characterisation," *J Drug Deliv Sci Tech,* vol. 39 pp. 180-191, 2017.

[57] R. Nair and A. K. Ck, "Formulation and characterization of famotidine loaded chitosan solid lipid nanoparticles for antiulcer activity," 2012.

[58] V. Kiessling, C. Wan, and L. K. Tamm, "Domain coupling in asymmetric lipid bilayers," *Biochimica et Biophysica Acta (BBA)-Biomembranes,* vol. 1788, pp. 64-71, 2009.

[59] E. Rascol, M. Daurat, A. Da Silva, M. Maynadier, C. Dorandeu, C. Charnay*, et al.*, "Biological fate of Fe3O4 core-shell mesoporous silica nanoparticles depending on particle surface chemistry," *Nanomaterials,* vol. 7, p. 162, 2017.

[60] D. Bhowmik, K. R. Mote, C. M. MacLaughlin, N. Biswas, B. Chandra, J. K. Basu*, et al.*, "Cell-membrane-mimicking lipid-coated nanoparticles confer Raman enhancement to membrane proteins and reveal membrane-attached amyloid-β conformation," *ACS nano,* vol. 9, pp. 9070-9077, 2015.

[61] N. M. Elbaz, I. A. Khalil, A. A. Abd-Rabou, and I. M. El-Sherbiny, "Chitosan-based nano-in-microparticle carriers for enhanced oral delivery and anticancer activity of propolis," *Int J Biol Macromol,* vol. 92, pp. 254-269, Nov 2016.

[62] J. Zhang, J. Li, Y. Ju, Y. Fu, T. Gong, and Z. Zhang, "Mechanism of Enhanced Oral Absorption of Morin by Phospholipid Complex Based Self-Nanoemulsifying Drug Delivery System," *Molecular Pharmaceutics,* vol. 12, pp. 504-513, 2015/02/02 2015.

[63] L. Maguire, M. Konoplyannikov, A. Ford, A. R. Maguire, and N. M. O'Brien, "Comparison of the cytotoxic effects of β-sitosterol oxides and a cholesterol oxide, 7β-hydroxycholesterol, in cultured mammalian cells," *British journal of nutrition,* vol. 90, pp. 767-775, 2003.

[64] K. Koschutnig, S. Heikkinen, S. Kemmo, A.-M. Lampi, V. Piironen, and K.-H. Wagner, "Cytotoxic and apoptotic effects of single and mixed oxides of β-sitosterol on HepG2-cells," *Toxicology in Vitro,* vol. 23, pp. 755-762, 2009.

[65] A. Z. Mirza and F. A. Siddiqui, "Nanomedicine and drug delivery: a mini review," *International Nano Letters,* vol. 4, pp. 1-7, 2014.

[66] J. K. Patra, G. Das, L. F. Fraceto, E. V. R. Campos, M. d. P. Rodriguez-Torres, L. S. Acosta-Torres*, et al.*, "Nano based drug delivery systems: recent developments and future prospects," *Journal of nanobiotechnology,* vol. 16, pp. 1-33, 2018.

[67] G. Cevc and H. Richardsen, "Lipid vesicles and membrane fusion," *Advanced Drug Delivery Reviews,* vol. 38, pp. 207-232, 1999.

[68] R. Kamel, "Nanotherapeutics as promising approaches to combat fungal infections," *Drug Development Research,* vol. 80, pp. 535-545, 2019.

[69] S. M. Jadhav, P. Morey, M. Karpe, and V. Kadam, "Novel vesicular system: an overview," *J. Appl. Pharm. Sci,* vol. 2, pp. 193-202, 2012.

[70] R. Kamel, "Contribution of Novel Delivery Systems in the Development of Phytotherapeutics," *Herbal Medicine: Back to the Future: Volume 4, Infectious Diseases,* vol. 4, p. 148, 2021.

[71] J. Zhang, Q. Peng, S. Shi, Q. Zhang, X. Sun, T. Gong*, et al.*, "Preparation, characterization, and in vivo evaluation of a self-nanoemulsifying drug delivery system (SNEDDS) loaded with morin-phospholipid complex," *International journal of nanomedicine,* vol. 6, pp. 3405-3414, 2011.

[72] L. Mei, Z. Zhang, L. Zhao, L. Huang, X.-L. Yang, J. Tang*, et al.*, "Pharmaceutical nanotechnology for oral delivery of anticancer drugs," *Advanced drug delivery reviews,* vol. 65, pp. 880-890, 2013.

[73] D. Stuart and T. Allen, "A new liposomal formulation for antisense oligodeoxynucleotides with small size, high incorporation efficiency and good stability," *Biochimica et Biophysica Acta (BBA)-Biomembranes,* vol. 1463, pp. 219-229, 2000.

Figure

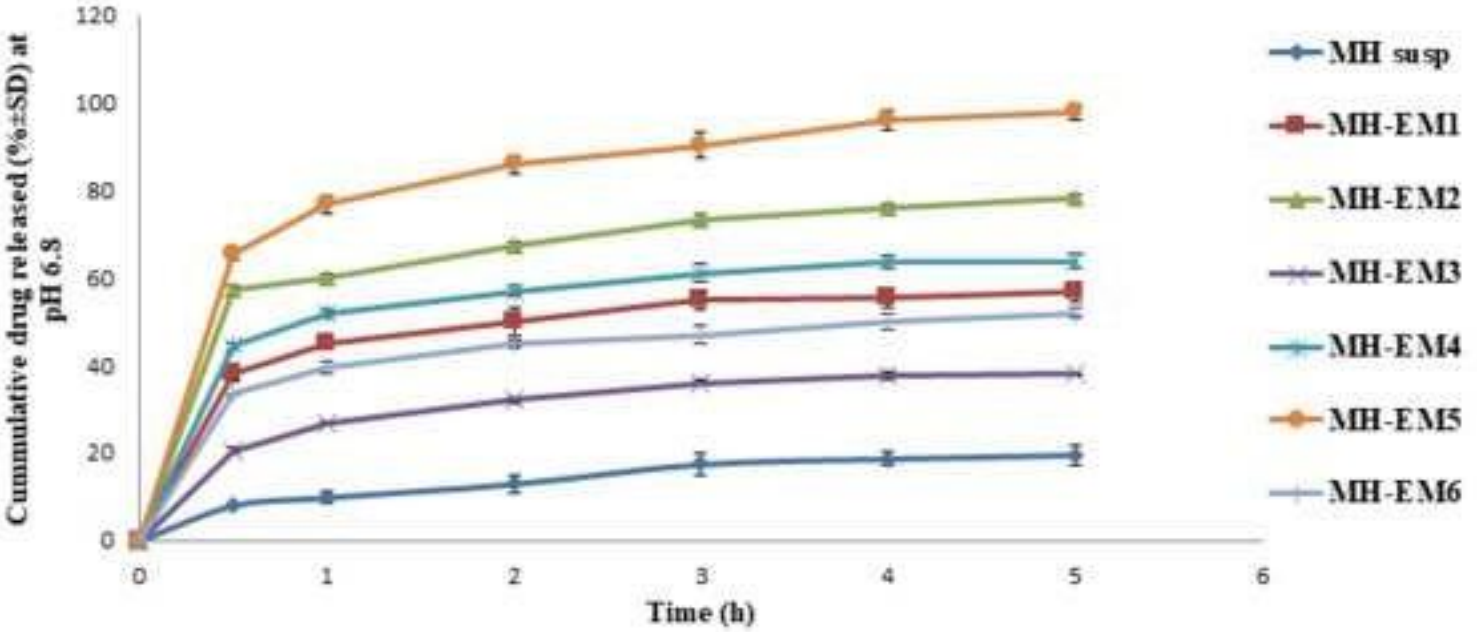
Cummulative drug released (%±SD) at pH 6.8
120
100
80
60
40
20
0
0
1
2
3
4
5
6
Time (h)
MH susp
MH-EM1
MH-EM2
MH-EM3
MH-EM4
MH-EM5
MH-EM6

(a)

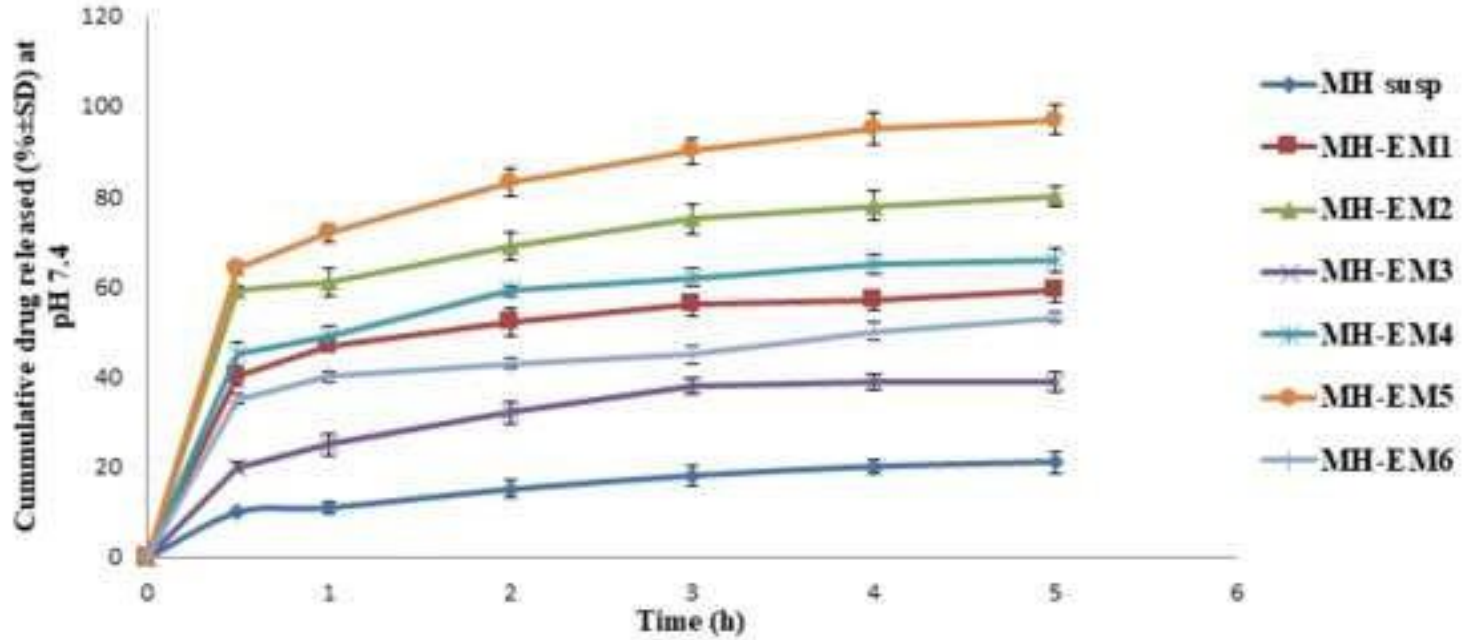
Cummulative drug released (%±SD) at pH 7.4
120
100
80
60
40
20
0
0
1
2
3
4
5
6
Time (h)
MH susp
MH-EM1
MH-EM2
MH-EM3
MH-EM4
MH-EM5
MH-EM6

(b)

Figure

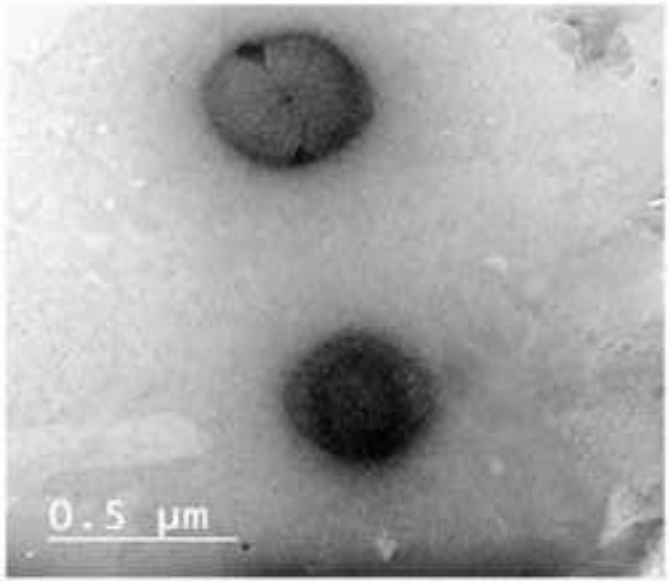
0.5 µm

(a)

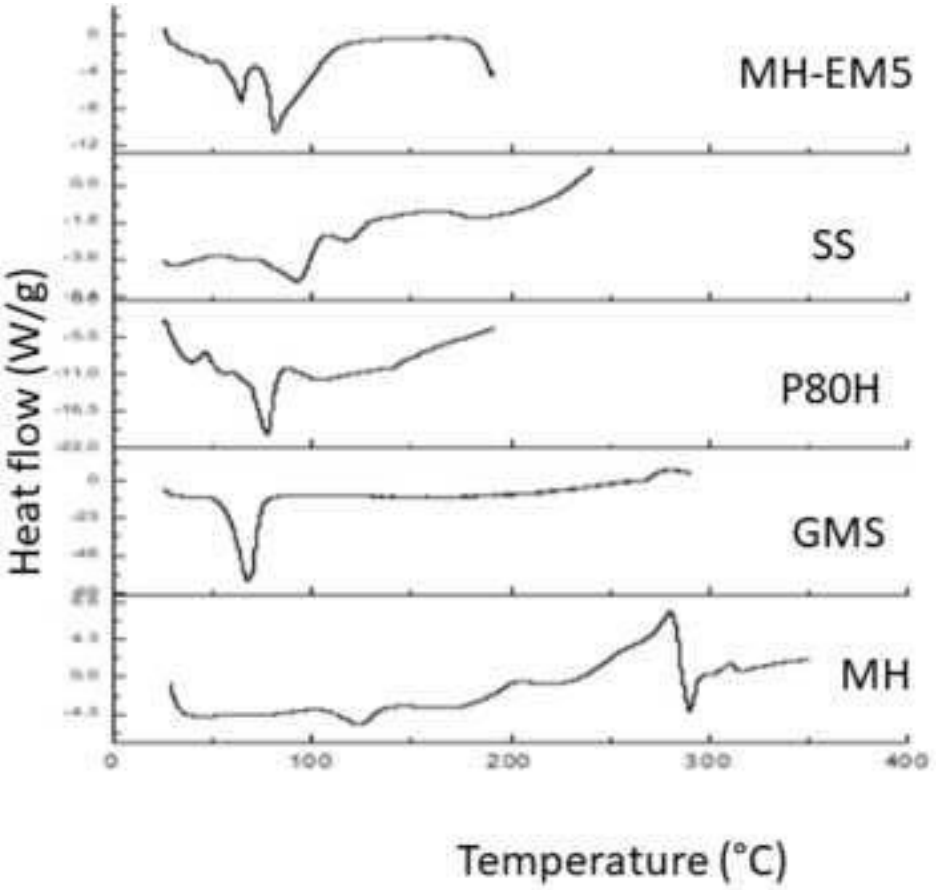
MH-EM5
SS
P80H
GMS
MH
Heat flow (W/g)
0
100
200
300
400
Temperature (°C)

(b)

Figure

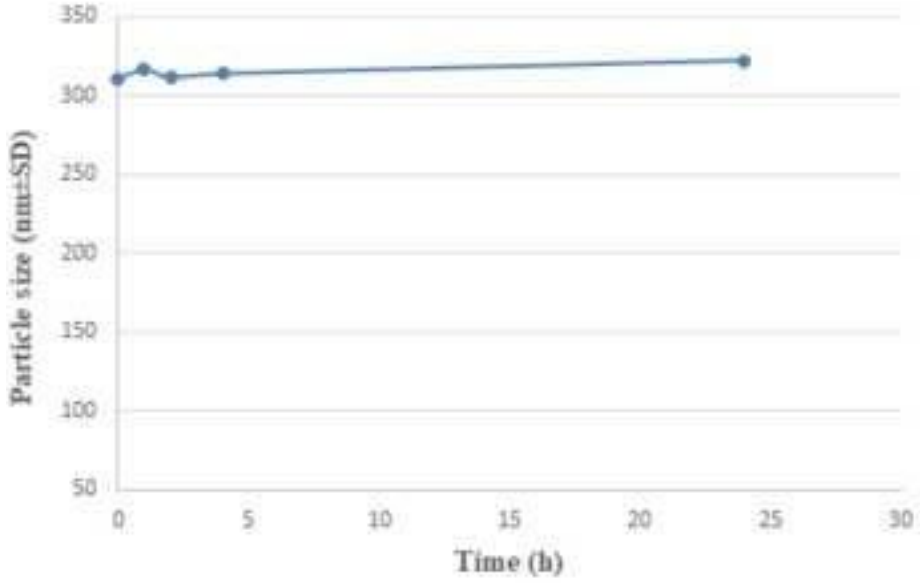
Particle size (nm±SD)
350
300
250
200
150
100
50
0
5
10
15
20
25
30
Time (h)

(a)

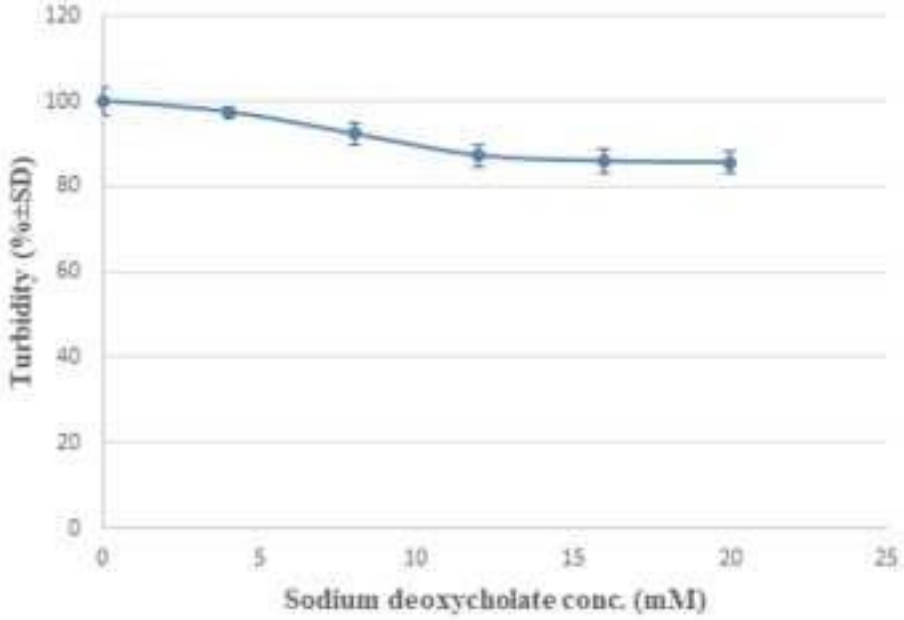
Turbidity (%±SD)
120
100
80
60
40
20
0
0
5
10
15
20
25
Sodium deoxycholate conc. (mM)

(b)

Figure

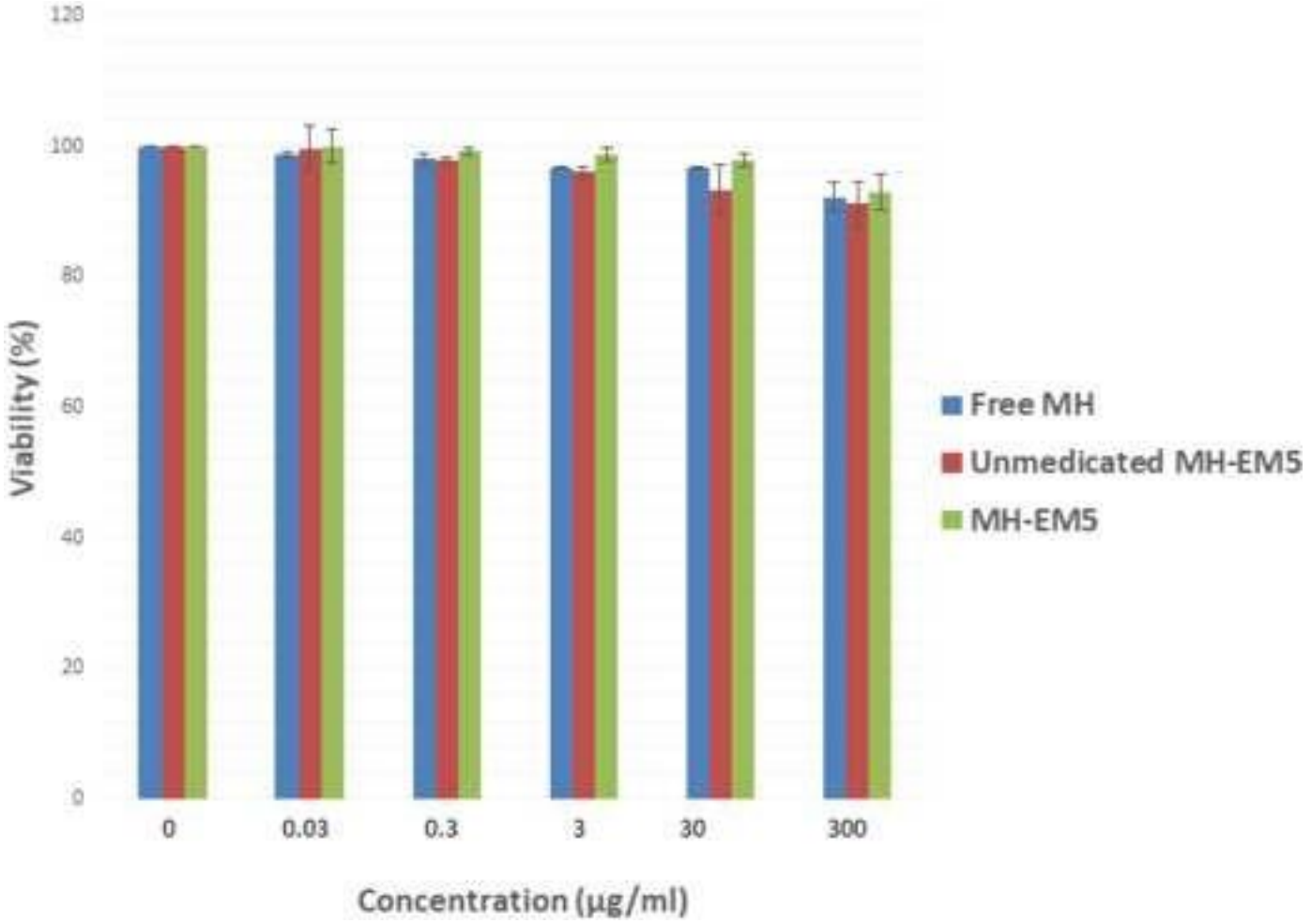
120
100
80
60
40
20
0
Viability (%)
0
0.03
0.3
3
30
300
Concentration (µg/ml)
Free MH
Unmedicated MH-EM5
MH-EM5

Figure

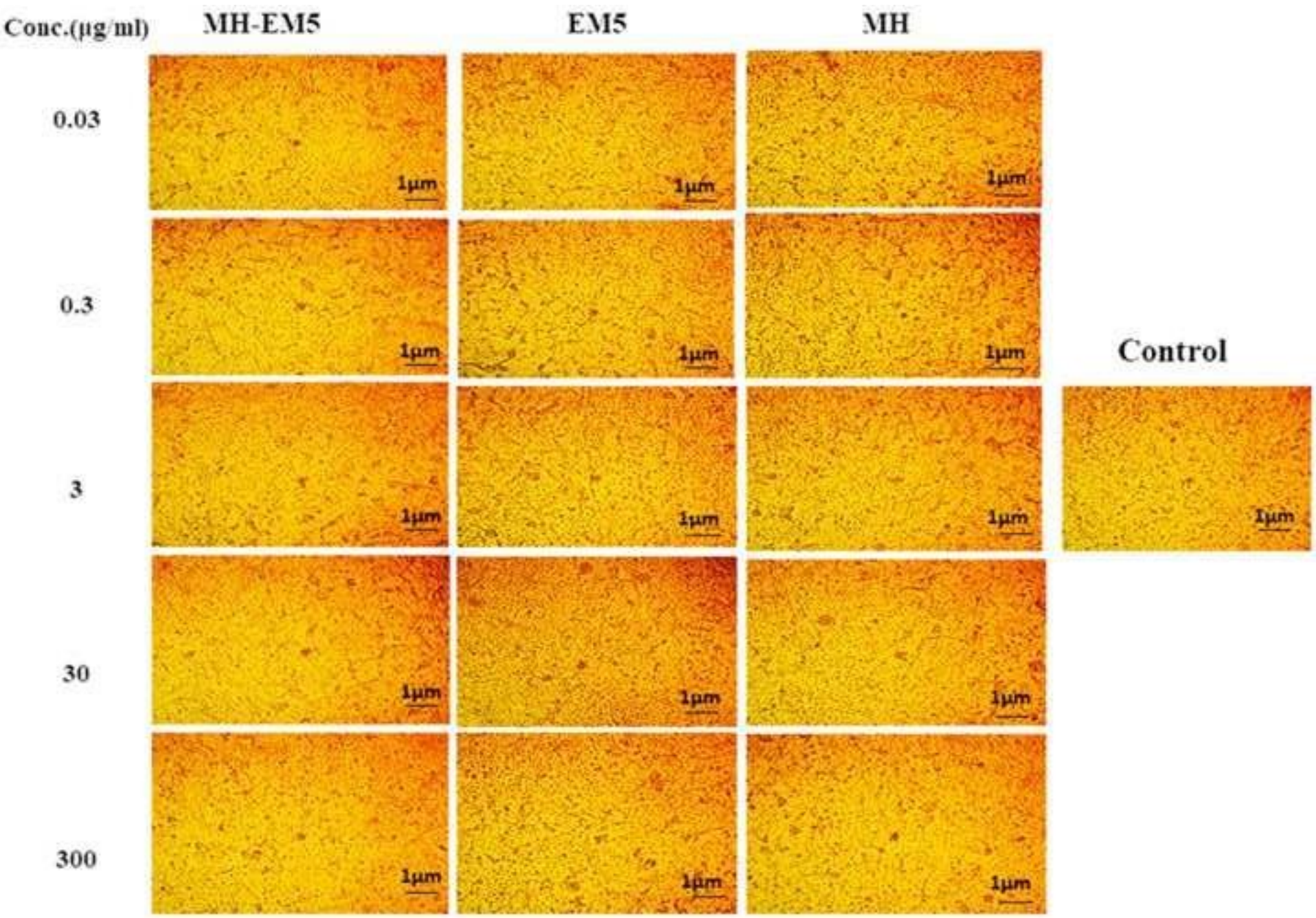

Figure

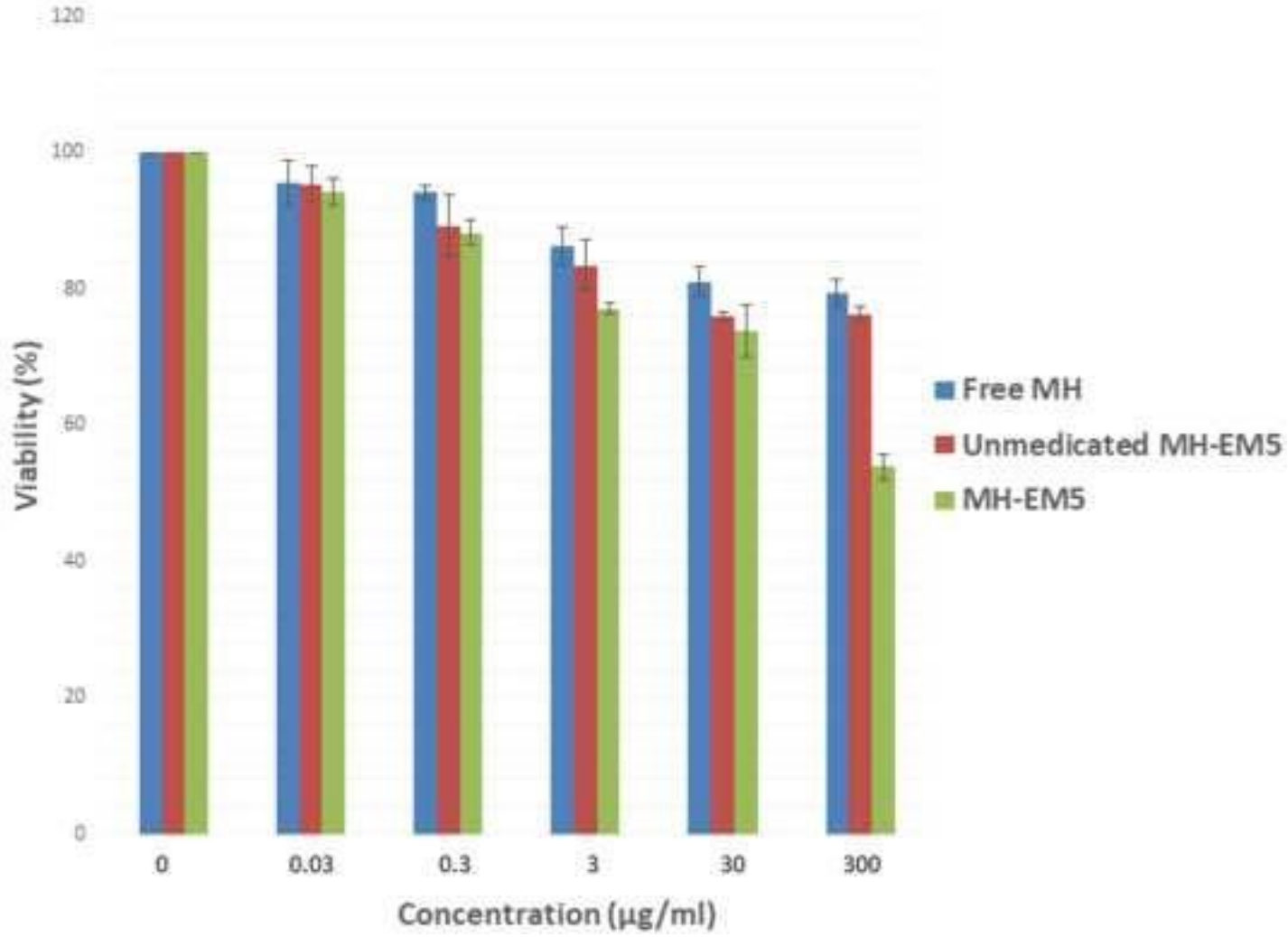
120
100
80
60
40
20
0
Viability (%)
0
0.03
0.3
3
30
300
Concentration (µg/ml)
Free MH
Unmedicated MH-EM5
MH-EM5

Figure

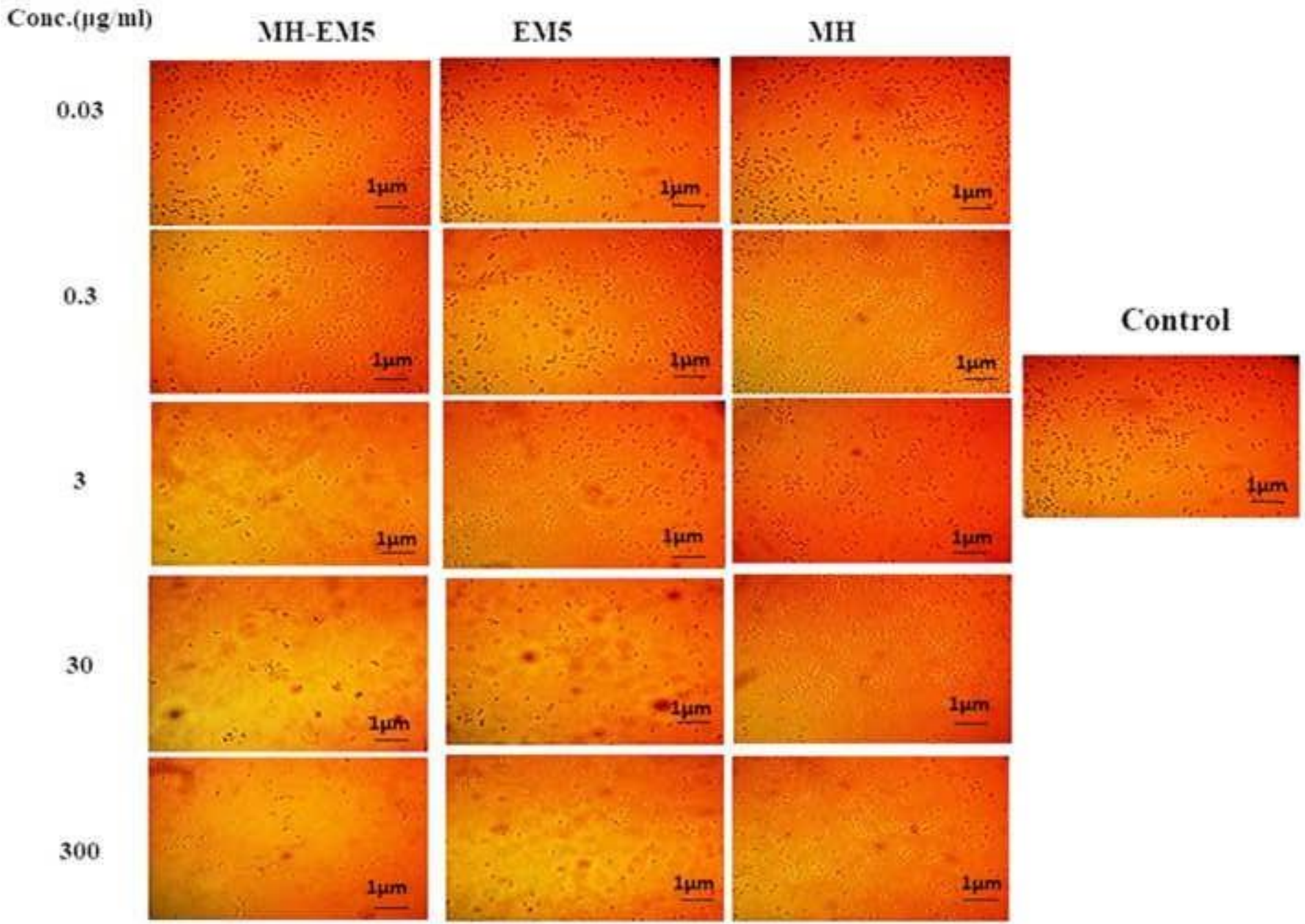

Figure

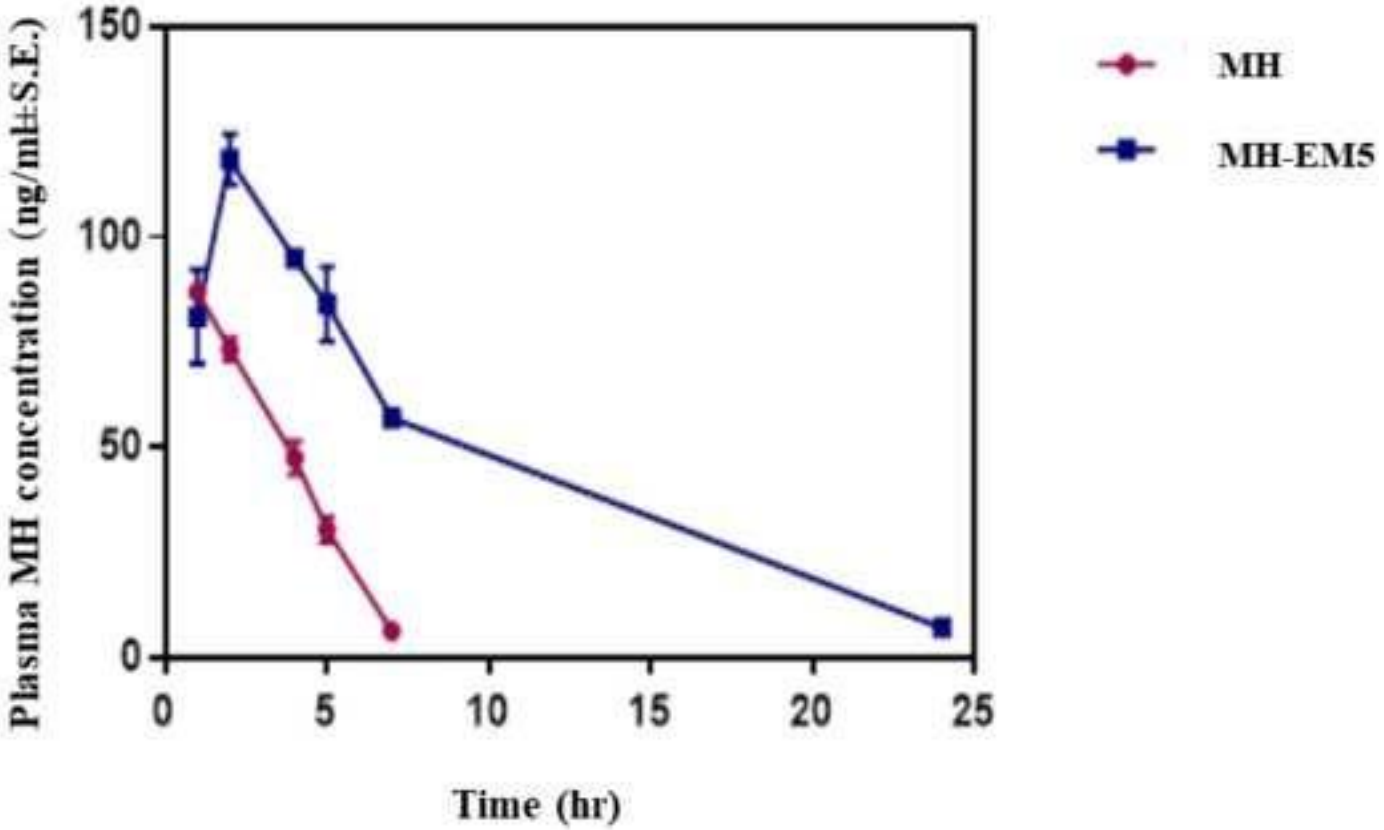
Plasma MH concentration (ng/ml±S.E.)
150
100
50
0
0
5
10
15
20
25
Time (hr)
MH
MH-EM5

Figure 1. In-vitro MH release profiles from different EMs formulations in phosphate buffer pH 6.8 (a) and 7.4 (b) at 37 °C. Each point represents the mean±SD,

Figure 2. (a) Transmission electron micrographs (TEM) of MH-EM5, and (b) DSC thermograms of MH (Morin hydrate), GMS (Glyceryl monostearate), P80H (Phospholipon 80H), SS (ß-sitosterol) and MH-EM5.

Figure 3. (a) Stability of MH-EM5 in serum, (b) Stability of MH-EM5 in bile salts.

Figure 4. Cytotoxicity effects of MH, EM5 and MH-EM5 against OEC after 48 h of incubation.

Figure 5. Microscopic photographs of the morphological changes induced by MH, EM5 and MH-EM5 on OEC cell lines after 48 h treatment compared to untreated control.

Figure 6. Cytotoxicity effects of MH, EM5 and MH-EM5 against AML cell lines after 48 h of incubation.

Figure 7. Microscopic photographs of the morphological changes induced by MH, EM5 and MH-EM5 on AML cell lines after 48 h treatment compared to untreated control.

Figure 8. Time course of MH in plasma of normal rats after single oral administration of MH and MH-EM5. Each data point represents the mean± S.E. of 6 rats.

Table

Formulations	Composition (ratio w/w)		
	GMS	P80H	SS
MH-EM1	1	1	-
MH-EM2	2	1	-
MH-EM3	1	2	-
MH-EM4	1	0.5	0.5
MH-EM5	2	0.5	0.5
MH-EM6	1	1	1

Table 1. Composition of the prepared drug-loaded emulsomes

Glyceryl monostearate (GMS)

Phospholipon 80H (P80H)

ß-sitosterol (SS)

Total amount of the ingredients = 100 mg

Formulations	EE%±SD	PS(nm±SD)	PDI±SD	ZP(mV)
MH-EM1	80.64±1.21	606.6±11.37	0.46±0.01	-33.1
MH-EM2	78.45±0.80	535.7±9.25	0.40±0.01	-34.2
MH-EM3	79.41±0.98	645.3±9.12	0.45±0.02	-34.0
MH-EM4	78.95±1.00	471.7±8.50	0.45±0.01	-36.2
MH-EM5	79.95±0.63	271.7±4.86	0.40±0.02	-37.3
MH-EM6	78.63±0.44	509.6±6.78	0.48±0.02	-37.5

Table 2. Particle size (PS), size distribution (PDI), Zeta potential (ZP), entrapment efficiency (EE) of the prepared MH-EMs

Formulations	RE	ER	Release kinetics (R^2)		
			Zero order	Higuchi order	First order
MH-EM1	**48.35±0.92**	**3.45**	**0.861**	***0.941***	**0.829**
MH-EM2	**65.92±1.61**	**4.70**	**0.954**	***0.986***	**0.941**
MH-EM3	**31.01±2.00**	**2.21**	**0.860**	***0.942***	**0.809**
MH-EM4	**54.91±1.46**	**3.92**	**0.863**	***0.943***	**0.832**
MH-EM5	**82.28±1.96**	**5.87**	**0.899**	***0.964***	**0.863**
MH-EM6	**42.87±1.43**	**3.06**	**0.906**	***0.968***	**0.867**
Drug susp.	**14.02±0.81**		**0.944**	***0.975***	**0.910**

Table 3(a). Release parameters for the MH- loaded emulsomes (MU-EMs) compared to the drug suspension (pH 6.8)

Release efficiency (RE)

Enhancement ratio (ER)= RE of MH-EM/RE of MH susp

Formulations	RE	ER	Release kinetics (R^2)		
			Zero order	Higuchi order	First order
MH-EM1	**49.95±1.92**	**3.25**	**0.872**	***0.949***	**0.837**
MH-EM2	**67.45±2.61**	**4.81**	**0.954**	***0.983***	**0.940**
MH-EM3	**31.45±2.90**	**2.24**	**0.861**	***0.939***	**0.825**
MH-EM4	**55.65±9.56**	**3.97**	**0.890**	***0.957***	**0.866**
MH-EM5	**80.50±2.96**	**5.74**	**0.928**	***0.983***	**0.901**
MH-EM6	**42.40±2.13**	**2.76**	**0.969**	***0.974***	**0.952**
Drug susp.	**15.35±1.51**		**0.964**	***0.986***	**0.933**

Table 3(b). Release parameters for the MH- loaded emulsomes (MU-EMs) compared to the drug suspension (pH 7.4)

	C_{max} (ng/mL)	T_{max} (hr)	t½ (hr)	AUC 0-∞ (ng.ml.h^{-1})	AUMC (ng.ml.h^{-1})	MRT (h)	Vz/F (mg/kg)(ng/ml)	CL/F (mg/kg)(ng/ml)	λz (h^{-1})
MH	73.3 ± 2.7	1 ± 0.0	2.73 ± 0.176	336.3 ± 8.6	965.1 ± 56.8	2.81 ± 0.076	0.041 ± 0.002	0.029 ± 0.0011	0.693 ± 0.018
MH-loaded EM	118.2* ± 5.8	2* ± 0.0	5.5* ± 0.68	1185*± 10.65	8760* ± 974.3	7.371* ± 0.76	0.065* ± 0.007	0.0084*± 0.000078	0.129* ± 0.014

Table 4. Pharmacokinetic parameters of MH and MH-loaded EM in normal rats

Cmax: peak plasma concentration

tmax : time to peak concentration

AUC0-∞: area under the plasma concentration-time curve

AUMC0-∞ : Area under the first moment curve

λz :elimination rate constant

t1/2: elimination half-life

MRT: mean residence time

Vz volume of distribution

Clearance (CL/F)